Crystallization-induced toughness of rubber-modified polylactide: combined effects of biodegradable impact modifier and effective nucleating agent

Jérémy Odent, Jean-Marie Raquez, Philippe Leclère, Franck Lauro, Philippe Dubois

Polymers for Advanced Technologies 26/7 (2015) 814-822

Crystallization-induced toughness of rubber-modified polylactide: combined effects of biodegradable impact modifier and effective nucleating agent

Jérémy Odent[a], Jean-Marie Raquez[a]*, Philippe Leclère[b], Franck Lauro[c] and Philippe Dubois[a]

a J. Odent, J.-M. Raquez, P. Dubois Laboratory of Polymeric and Composite Materials (LPCM), Research Insti-tute for Materials Science and Engineering, Center of Innovation and Research in Materials and Polymers (CIRMAP), University of Mons, Place du Parc 23, B-7000 Mons, Belgium

b P. Leclère Laboratory of Chemistry of Novel Materials (CMN)), Research Institute for Materials Science and Engineering, Center of Innovation and Research in Materials and Polymers (CIRMAP), University of Mons, Place du Parc 23, B-7000 Mons, Belgium

c F. Lauro Industrial and Human Automatic Control and Mechanical Engineering Laboratory (LAMIH), CNRS Research Unit, MECAMAT, CSMA, University of Valenciennes and Hainaut-Cambresis, Le Mont Houy, BP 311, 59304 Valenciennes Cedex, France

ABSTRACT

The co-addition of rubber-like poly(ε-caprolactone-*co*-D,L-lactide) (P[CL-*co*-LA]) as impact modifier and *N,N′*-ethylenebis(stereamide) (EBS) as nucleating agent has here been investigated to tailor both the crystallization and toughness of resulting polylactide (PLA)-based materials. In this work, 10 wt% of P[CL-*co*-LA] copolymer and different concentrations of EBS were added into PLA by twin-screw extrusion (in a micro-compounder) in order to establish the mechanical performances of the resulting blends upon the nucleating agent content. Crystallization behavior and impact toughness of PLA-based materials were both enhanced and were ascribed to a clear alteration of the matrix crystallinity, spherulitic growth rate, and crystal structure upon the nucleating agent content. As a result, toughness of PLA-based materials was considerably enhanced up to, at least, 11 times with respect to neat PLA. Such improvement of the fracture resistance upon the extent of PLA crystallinity was related to a change in the toughening mechanism from crazing to shear-yielding (combined with crazing) through the deformation of spherulites, promoting high energy dissipation pathways as crystallization occurs.

Keywords: Polylactide; impact modifier; nucleating agent; crystallinity; toughening mechanisms

INTRODUCTION

With increasing concerns about environmental and sustainability issues, polylactide (PLA) has gained much attention in recent years as a biodegradable polymer produced from renewable re-sources.[1,2] The reason for its development relies mainly on a number of interesting properties, including its good processabil-ity, good mechanical properties, biocompatibility, and renew-ability.[3,4] However, in many cases, the practical applications of PLA have been significantly impaired by its inherent brittleness related to low Izod impact strength of ca. 2.7 kJ/m^2[5,6] In this re-gard, extensive efforts have been made to reduce the brittleness of PLA for its industrial implementation in some areas, such as packaging, automotive, and electronic industries.[7,8] Some works were also performed to promote energy dissipation and toughness through the crystallization of PLA matrix.[9–12] From these studies, the increase of PLA crystallinity upon annealing treatments[13–16] or the addition of nucleating agents[17–20] was reported as decisive in the toughening of PLA-based materials. For instance, different trends of fracture behavior upon testing speeds and annealing conditions were reported within annealed PLA by Park et al.[13] and Nascimento et al.[14] This revealed a sig-nificant improvement of the fracture toughness upon the extent of crystallinity, which had been related to the formation of duc-tile fibrils through the deformation of spherulites under stress as crystallinity increases. Indeed, a much more effective energy dissipation regarding two possible structures is reached within crystalline zones, which are the inter-spherulitic crack growth and the crack growth through spherulites.[13,21] Semi-crystalline polymers usually exhibit a typical structure consisting of closely packed crystalline lamellae separated by amorphous regions.

DOI : 10.1002/pat.3513

When the blend is subjected to an external impact force, the fracture energy is dissipated through shear yielding in the crystalline zones and crazing in the amorphous zones. Accordingly, the extent of plastic deformation induced in crystalline polymers gives rise to a largely improved impact toughness through a change in the deformation mechanism from crazing to shear yielding as crystallization occurs.[22]

For L-lactide-enriched PLA, its crystallization rate is quite low, and the use of highly active nucleating agents represents a promising way to remarkably accelerate the crystallization of PLA matrix.[23,24] Many researchers have thereby investigated the combination of both active nucleating agent and impact modifier as an effective method to simultaneously improve the crystallization and the impact toughness of PLA.[25–28] In this respect, Jain *et al.*[29] investigated talc loading on phase morphology and resulting properties of PLA/poly(ε-caprolactone) (PCL) immiscible blends. They found that talc not only acted as a nucleating agent, but also improved the miscibility and adhesion between the dispersed phase and the matrix, which in turn allow the toughening of the overall materials. A suitable particle size for impact modifiers is another precondition for highly crystalline matrix to work effectively in the toughening of resulting matrix/impact modifier blends.[15,26,30] In this respect, Bai *et al.*[25,26] identified an evident decrease of optimum particle size for toughening PLA/PCL blends as the crystallinity of the PLA matrix increases. It is worth noting that shear yielding is a much more effective energy dissipative micromechanism with respect to crazing, which is often encountered in small rubbery microdomains (i.e., $<0.5\ \mu m$).[31–33] This so implies an efficient path for the propagation of shear-yielding deformation needed for effective impact energy absorption upon the combined roles of matrix crystallization and impact modifier particle size. Oyama *et al.*[15] significantly improved the toughness of PLA/EGMA (80/20 wt/wt) blends from 5.5 to 72 kJ/m^2 upon the increase of PLA crystallinity from 5% to 40% and an optimum microdomain size range of 0.3–0.5 μm. From these investigations, the increase of PLA crystalline content can be viewed as a promising way to enlarge plastic deformation throughout the matrix, thus causing high toughening performance.

The present contribution aims at tailoring the material toughness upon the combination of both highly effective nucleating agent and impact modifier within PLA. Recently, we have reported the use of as-synthesized hydrolytically degradable poly(ε-caprolactone-*co*-D,L-lactide) (P[CL-*co*-LA]) copolymers as effective biodegradable impact modifiers for PLA.[34] Another recent contribution by Murariu *et al.* highlighted *N,N'*-ethylenebis(stereamide) (EBS), a selected fatty amide able to promote lubrication and chain mobility during PLA crystallization as a remarkable nucleating agent for PLA.[35] In this respect, the co-addition of 10 wt% of P[CL-*co*-LA] impact modifier and different concentrations of EBS nucleating agent was investigated on the outstanding crystallization properties (i.e., crystallinity degree, spherulitic growth rate, and crystal structure) and the overall material performances. Finally, this work is made to discuss the close relationship between the extent of PLA crystallinity and the recorded synergistic toughness effect within these resulting PLA-based materials. The contribution of which was thereby investigated by means of thermal, mechanical, and morphological methods. A toughening mechanism related to the final mechanical performances was finally proposed to account for the impact behavior of the as-produced PLA-based materials.

EXPERIMENTAL SECTION

Materials

The ε-caprolactone (99%, Acros, Geel, Belgium) was dried for 48 h over calcium hydride and distilled under reduced pressure. D,L-lactide (>99.5%, Purac, Gorinchem, The Netherlands) was conserved in a glove box. *n*-heptanol (98%, Aldrich, Darmstadt, Germany) was dried over a molecular sieve (4 Å), and tin(II) octoate ($Sn(Oct)_2$) (95%, Aldrich) was used as received without any purification and diluted in dry toluene (0.01 M). A commercially available extrusion-grade PLA (NatureWorks 4032D, Nebraska, USA) designed especially for biaxially oriented films was used as received ($\overline{M_n}$ =133,500 ± 5000 g/mol, Đ = 1.94 ± 0.06 as determined by size-exclusion chromatography using (relative to polystyrene calibration), 1.4 ± 0.2% D-isomer content as determined by the supplier). *N,N'*-ethylene bis(stereamide) (EBS) is a commercial polymer additive from Aldrich. CAB-O-SIL M-5 (SiO_2, 200 m^2/g) is untreated fumed silica, supplied by Cabot (Cabot, Massachusetts, USA), and is used as received.

Synthesis of poly(ε-caprolactone-co-D,L-lactide) copolymer

The copolymerization was carried out in bulk by ring-opening polymerization of ε-caprolactone and D,L-lactide promoted by *n*-heptanol and tin(II) octoate for an initial molar [alcohol]/[tin(II) octoate] ratio of 100. The reaction was carried out for 24 h in an oil bath at 160°C and stopped by quenching it in an ice bath. The crude product was dissolved in a minimum volume of chloroform, followed by precipitation into a 10-fold excess of heptane. They were recovered after filtration and dried under vacuum until reaching a constant weight. The molar LA content of the resulting copolymer was of 28 mol% (as determined by Proton nuclear magnetic resonance [^{1}H NMR] analyses), while the number-average molecular weight was of 35,400 g/mol (equivalent polystyrene), together with a dispersity index of 2.0 (as determined by gel permeation chromatography analysis). The so-synthesized copolymer proved totally amorphous and was characterized by a low glass transition temperature of around −36°C (as determined by differential scanning calorimetry [DSC] analysis).

Sample preparation and compounding

For safety reasons, a two-step process was carried out to prepare PLA/P[CL-*co*-LA]/EBS blends. PLA/EBS masterbatches were prepared by solvent casting using chloroform and dried for at least 12 h at 80°C under reduced pressure (10^{-1} mbar), in order to remove any residual organic solvent and water. The resulting masterbatch was subsequently melt-blended in the presence of 10 wt% P[CL-*co*-LA] copolymer (previously dried for at least 12 h at room temperature under reduced pressure) using a DSM twin-screw micro-compounder (15 cc) at 200°C and 60 rpm for 3 min. For the sake of comparison, the simple blend exclusively made of PLA and P[CL-*co*-LA] copolymer was prepared using a DSM twin-screw micro-compounder (15 cc) at 200°C and 60 rpm for 3 min, starting directly from PLA pellets (previously dried for at least 12 h at 80°C under reduced pressure) and 10 wt% P[CL-*co*-LA] copolymer (previously dried for at least 12 h at room temperature and under reduced pressure of 10^{-1} mbar). For tensile and impact characterizations, the PLA-based materials were prepared by compression molding at 200°C for 10 minutes. Further PLA/P[CL-*co*-LA]/SiO_2/EBS blends were prepared following the same two-step process in which SiO_2 and EBS were previously dispersed within the PLA matrix by solvent casting using chloroform. As in the preceding

discussion, the resulting PLA/SiO_2/EBS masterbatch was subsequently melt-blended in the presence of 10 wt% P[CL-*co*-LA] copolymer using a DSM twin-screw micro-compounder (200°C, 60 rpm, 3 min) and both compression molding (200°C, 10 min) or injection molding (200°C, 3 min, 9 bars).

Characterization techniques

Proton nuclear magnetic resonance spectra were recorded in $CDCl_3$ using a Bruker AMX-500 apparatus (Billerica, MA, USA) at a frequency of 500 MHz. Size-exclusion chromatography was performed in THF (containing 2 wt% NEt_3) or in chloroform (sample concentration: 1 wt%) at 35°C, using a polymer laboratories (PL) liquid chromatography equipped with a PL-DG802 degazer, an isocratic high-performance liquid chromatography pump LC1120 (flow rate: 1 mL/min), a Basic-Marathon Autosampler, a PL-RI refractive index detector (Agilent Technologies, Cheadle, England) and four columns: a guard column PLgel 10 μm (50 × 7.5 mm) and two columns PLgel mixed-B 10 μm (300 × 7.5 mm). Molecular weight and molecular weight distribution were calculated by reference to a relative calibration curve made of polystyrene standards. DSC was performed using a DSC Q2000 from TA Instruments (Newcastle, DE, USA) at heating and cooling rates of 10°C/min under nitrogen flow (2nd scan). Notched Izod impact tests were performed according to ASTM D256 (Benelux Scientific, Eke, Belgium) using a Ray-Ran 2500 pendulum impact tester (E = 4 J, mass = 0.668 kg, and speed = 0.46 m/s). Tensile tests were performed according to ASTM D638 using a Zwick universal tensile testing machine (Ulm, Germany) (speed = 1 mm/min and preload = 5 N). Dynamic mechanical thermal analyses (DMTA) were performed under ambient atmosphere using a DMTA Q800 apparatus from TA Instruments in a dual cantilever. The measurements were carried out at a constant frequency of 1 Hz, a temperature range from −100°C to 150°C at a heating rate of 2°C/min. Data acquisition and analysis of the storage modulus (E'), loss modulus (E''), and loss tangent (tan δ) were recorded automatically by the system. Polarized optical microscopy was used to study the spherulitic growth rate and crystal morphology. Accordingly, samples sandwiched between two glass slides were heated on Linkam THMS 600 hot stage (Linkam Scientific Instruments, Ltd., Surrey, UK) from room temperature to 200°C at a rate of 30°C/min, held at this temperature for 5 min before being cooled at the same rate to 150°C (crystallization initiates before reaching temperature below 150°C). They were then held isothermally for different periods of time during which images were taken using Leica DM LM/p (Leica microsystems, Wetzlar, Germany) polarized optical microscope. Transmission electron microscopy (TEM) was carried out using a Philips CM20 microscope (FEI, Eindhoven, The Netherlands) operated at 200 kV to investigate the morphological structure of resulting materials. Atomic force microscopy (AFM) was carried out on a Bruker Dimension Icon using Tapping Mode and a new AFM technique called peak-force tapping (PFT) based on real time-force distance curve analysis recorded at a frequency of about 2 kHz.[36] For both TEM and PFT-AFM images, the samples were cryomicrotomed at −100°C by a Leica UCT microtome before imaging. Room-temperature impact-fractured surfaces of specimens were sputter coated with gold and then examined through scanning electron microscopy (SEM) to highlight plastic deformation and possible toughening mechanisms. Accordingly, the room-temperature fracture was performed with a single-column tensile test machine type Hounsfield H5KT (Tinius Olsen, USA, Pennsylvania) with 5kN cell force at a speed of 1 mm/min, while SEM analyses were carried out using a Hitachi SU8020 (Hitachi, Tokyo, Japan) (100 V–30 kV).

RESULTS AND DISCUSSION

A challenge to simultaneously improve PLA crystallization and PLA toughness is appealing. Following this objective, we first considered the effect of EBS nucleating agent on the crystallinity extent of PLA/P[CL-*co*-LA] (90/10 wt/wt) blends using DSC, a simple technique giving relevant information about the crystallization properties through isothermal and non-isothermal measurements. Using the isothermal crystallization experiments, the determination of the crystallization half-time ($t_{1/2}$) commonly attests the effectiveness of nucleating agents.[17,24] Selected data obtained from the isothermal crystallization at 110°C of resulting PLA-based materials are accordingly shown in Fig. 1. Neat PLA had a long half-crystallization time ($t_{1/2}$ around 28 min), attesting for its low crystallization kinetics. However, its overall crystallization rate is reduced ($t_{1/2}$ around 5 min) when processed, resulting to a shear-induced crystallinity.[37] These results are in good agreement with the values currently reported in literature.[18,24] In a good agreement, the addition of P[CL-*co*-LA] impact modifier into the matrix led to lower $t_{1/2}$ with respect to neat PLA (Fig. 1). Similar results were reported by Sakai *et al.*,[38] assuming that PCL-based dispersed phase acted as active sites for nucleation. The limited miscibility between PLA and P[CL-*co*-LA] impact modifier and the locally activated chain mobility at the interface is thereby responsible for this remarkable enhancement of the PLA nucleation. Furthermore, it is believed that the EBS additive plays a complex role in the crystallization of PLA, promoting nucleation and chain mobility. As a result, intense and narrow exotherms are recorded in the presence of EBS (Fig. 1). The nucleated PLA/P[CL-*co*-LA] materials containing EBS show significant reductions about $t_{1/2}$ (too fast to be accurately determined), confirming that EBS behaves as a remarkable nucleating agent for PLA-based materials.

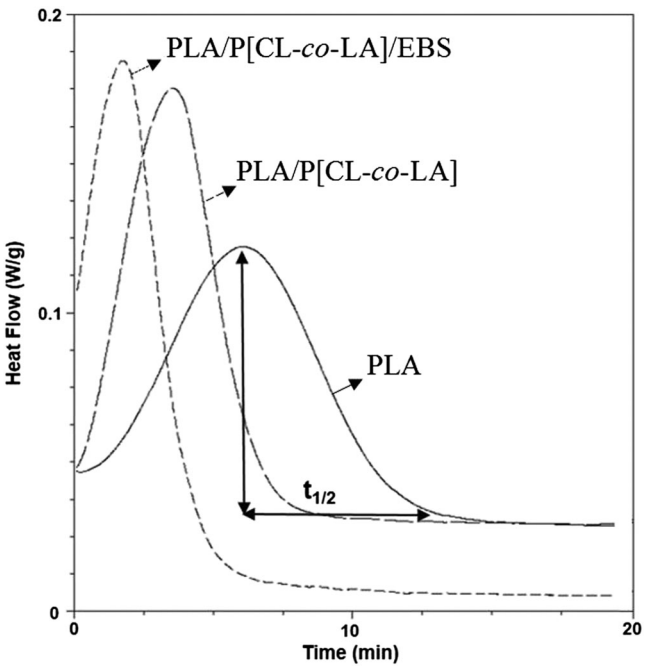

Figure 1. Differential scanning calorimetry thermograms of the isothermal crystallization (cooled from melt to 110°C) of neat polylactide (PLA) (line), PLA-based materials containing 10 wt% of P[CL-*co*-LA] (long dash) and corresponding blends filled with 4 wt% of EBS (short dash).

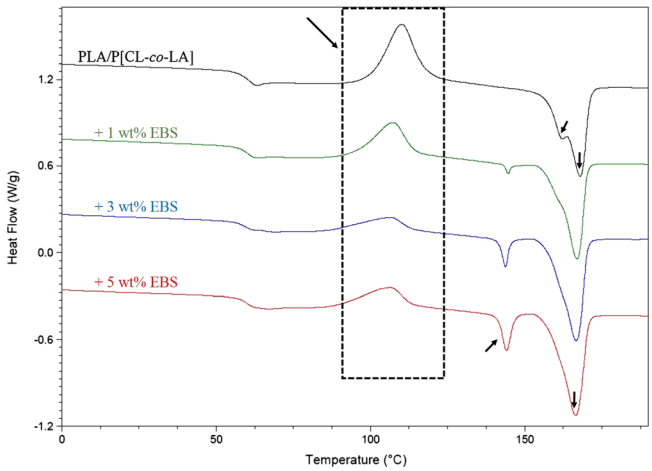

Figure 2. Non-isothermal differential scanning calorimetry thermograms of polylactide-based materials containing 10 wt% of P[CL-*co*-LA] (black) and corresponding blends filled with 1 wt% (green), 3 wt% (blue), and 5 wt% (red) of EBS. This figure is available in colour online at wileyonlinelibrary.com/journal/pat

Another confirmation comes from the non-isothermal DSC profiles and corresponding data of resulting PLA-based materials with increasing EBS concentrations (Fig. 2). As expected, the melting (T_m) and glass transition (T_g) temperatures of resulting PLA-based materials remained unchanged at *ca*. 168°C and 61°C, respectively, upon the addition of EBS. However, a new endothermic peak that can be reasonably ascribed to the melting of EBS is identified at around 145°C, the extent of which greatly increased with the EBS concentration. The observation of a cold crystallization exotherm (T_c) on heating prior to the melting endotherm (i.e., around 110°C) usually assert to the low crystallization rate of PLA-based materials. From this study, the significant decrease of the cold crystallization enthalpy (ΔH_c) was assigned to a gain of crystallinity upon the addition of EBS within these PLA/P[CL-*co*-LA] blends (Table 1S, *Supporting Information*). Further evidence is provided by the DSC cooling scans, whereas addition of EBS within PLA-based materials gave rise to an exothermic crystallization peak on cooling (results not shown). As far as PLA melting is concerned, multiple melting peaks are usually ascribed to different crystalline structures, that is, crystalline regions of various size and perfection.[39–41] For instance, the less stable α' crystal form is known to exist at lower temperatures than the α-form within PLA.[42] As a result, the appearance of a double melting peak is observed for neat PLA and the corresponding PLA/impact modifier blend. In contrast, the addition of EBS into PLA/P[CL-*co*-LA] blends led to a single T_m (i.e., no multiple melting peaks), relating to an alteration in the crystallization behavior (Fig. 2). Similar trends were reported by, for example, Murariu *et al.*, following the evaluation of PLA/nanofiller/EBS nanocomposites.[35] Even if the crystallinity degree of PLA-based blends increased from 3% to 13% after adding 10 wt% of P[CL-*co*-LA] copolymer within PLA, no noticeable changes in crystallinity degree was reported in the presence of EBS (Table1S, *Supporting Information*). A possible explanation may arise from the localization of a fraction of EBS nucleating agent within the P[CL-*co*-LA] dispersed phase, decreasing the available EBS content towards the PLA crystallization. It is worth reminding that semi-crystalline polymers like PLA exhibit a remarkably complex solid-state structure in which its crystallinity extent depends on, for example, crystallization temperature, optical purity, molecular weight, processing parameters, and so on.[43] Even at the same crystallinity extent, other effects on the crystallinity and related material performances may be obtained due to, for example, different lamellar organizations, crystalline form, or crystal structure. For instance, Cocca *et al.* reported difference of properties between PLA α and α' crystal forms,

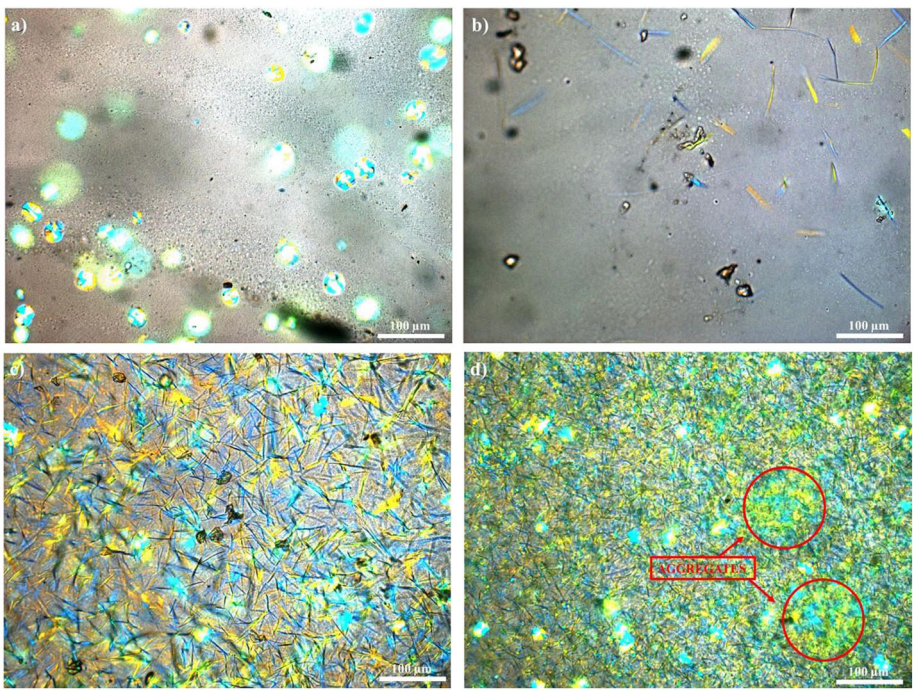

Figure 3. Polarized optical microscopy micrographs of polylactide-based materials containing 10 wt% of P[CL-*co*-LA] (a) and corresponding blends filled with 1 wt% (b), 3 wt% (c), and 5 wt% (d) of EBS following crystallization from melt at 150°C (images after 15 min under isotherme). This figure is available in colour online at wileyonlinelibrary.com/journal/pat

highlighting higher Young's modulus but lower elongation at break in the α-form. This was related to its more ordered and more densely packed crystal structure compared with α' form.[42] In this respect and to understand the effect of the incorporation of EBS nucleating agent on the crystal structures of these PLA-based materials, morphological investigations were carried out.

The crystal morphologies of such PLA/P[CL-*co*-LA]-based blends upon the EBS concentration were observed through POM analysis (Fig. 3) and related spherulitic growth rate study (Table 2S, *Supporting Information*). At a crystallization temperature of 150°C (i.e., the lowest temperature to avoid the matrix crystallization before reaching the isotherm), the nuclei density and the spherulitic growth rate were quite low, and only few spherulites could be observed for neat PLA (not shown). In contrast, smaller spherulites which grew faster (with an initiation time of only 4 min 30 s, see Table 2S, *Supporting Information*) are observed in the PLA/P[CL-*co*-LA] binary blend (Fig. 3(a)). It can be therefore stated out that the nuclei density of the PLA matrix has been greatly enhanced by the presence of P[CL-*co*-LA] impact modifier with respect to neat PLA. This is well consistent with the aforementioned DSC results. Interestingly, numerous tiny crystals that have impinged on each other were formed upon the addition of EBS into the PLA/P[CL-*co*-LA] blends. This results in a large increased nuclei density and a faster spherulitic growth rate in the presence of EBS (e.g., initiation time of only 20 s at 4 wt% of EBS, see Table 2S, *Supporting Information*). More surprisingly, an alteration of the crystal structure was reported in the presence of EBS nucleating agent, passing from large spherical crystals to tiny elongated and entangled ones (Fig. 3). The occurrence of such elongated crystals clearly resulted from the natural ribbon shape of EBS nucleating agent (as attested by TEM, see Figure 1S, *Supporting Information*), while their entanglements and their growth thereby took part in the large nuclei density achieved upon the EBS content. Indeed, more densely nucleated crystals and drastically faster spherulitic growth rate are reached by increasing the EBS concentration within PLA/P[CL-*co*-LA] blends (Fig. 3). However, it is worth noting that further increasing the EBS content up to 4 wt% did not promote a larger extent of entanglement but led to the main aggregation of as-formed crystals within the blends (Fig. 3(d)). This new crystal structure appears as a promising way to endow PLA-based materials with new physical properties and toughening through an effective path for the propagation of energy-dissipative mechanisms.

The significant change in crystal morphology of the nucleated blends is expected to affect the material performances. For instance, Grein *et al.*[44] reported changes in micro-deformation mechanisms upon the crystal structure, showing that, for example, large spherulites often promote brittleness due to the concentration of structural defects and impurities at their boundaries. Accordingly, tensile and impact properties of the as-produced PLA-based materials have been determined and compared with neat PLA and non-nucleated PLA/P[CL-*co*-LA] binary blend (Fig. 4). While neat PLA is viewed as a stiff and brittle material displaying a high Young's Modulus of *ca*. 1860 MPa and an impact strength of *ca*. 2.7 kJ/m^2, loading 10 wt% of P[CL-*co*-LA] copolymer into PLA leads to a brittle-ductile transition for the resulting blend characterized by a four-fold increase in toughness (*ca*. 11.4 kJ/m^2), together with a slight decrease in Young's modulus (*ca*. 1680 MPa). Interestingly enough, the change of the crystal structure induced by the presence of EBS within the rubber-toughened PLA/P[CL-*co*-LA] blends provided a significant increase, up to 10-fold, in the impact strength (Fig. 4). For instance, loading 4 wt% of EBS within PLA/P[CL-*co*-LA] (90/10 wt/wt) blend triggered an increase in impact strength by a factor of 11.3 (i.e., 30.5 kJ/m^2 with respect to 2.7 kJ/m^2 for neat PLA). Furthermore, the tensile properties of resulting PLA-based materials were not altered upon the addition of EBS, and the Young's modulus was even slightly enhanced mediated by the so-induced crystallization (Table 3S, *Supporting Information* for additional details). Directly related to the crystallinity extent and the crystal structure changes, a gradual increase in the overall toughness upon the EBS content is reached, imparting a maximum at 4 wt% of EBS (Fig. 4). At this stage, it can be claimed out that the growth of a more densely nucleated structure made of elongated and entangled crystals affords a more efficient toughening pathway. However, once a higher loading of nucleating agent was used, actually higher than 4 wt% of EBS, a drop in the toughness of resulting PLA-based blends occurs in relation to the presence of crystalline aggregates within the PLA-based blends (see Fig. 3 as a reminder).

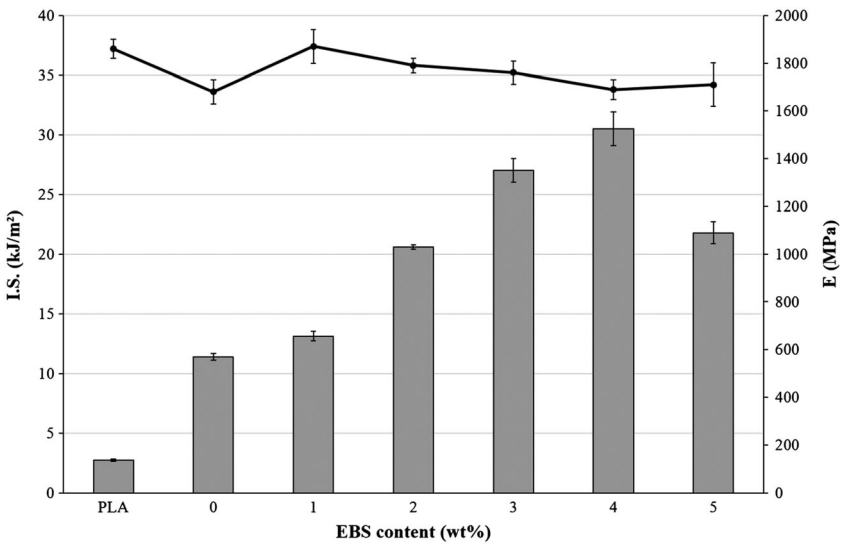

Figure 4. Notched Izod impact strength and Young's modulus of polylactide-based materials containing 10 wt% of P[CL-*co*-LA] copolymer upon the addition of EBS.

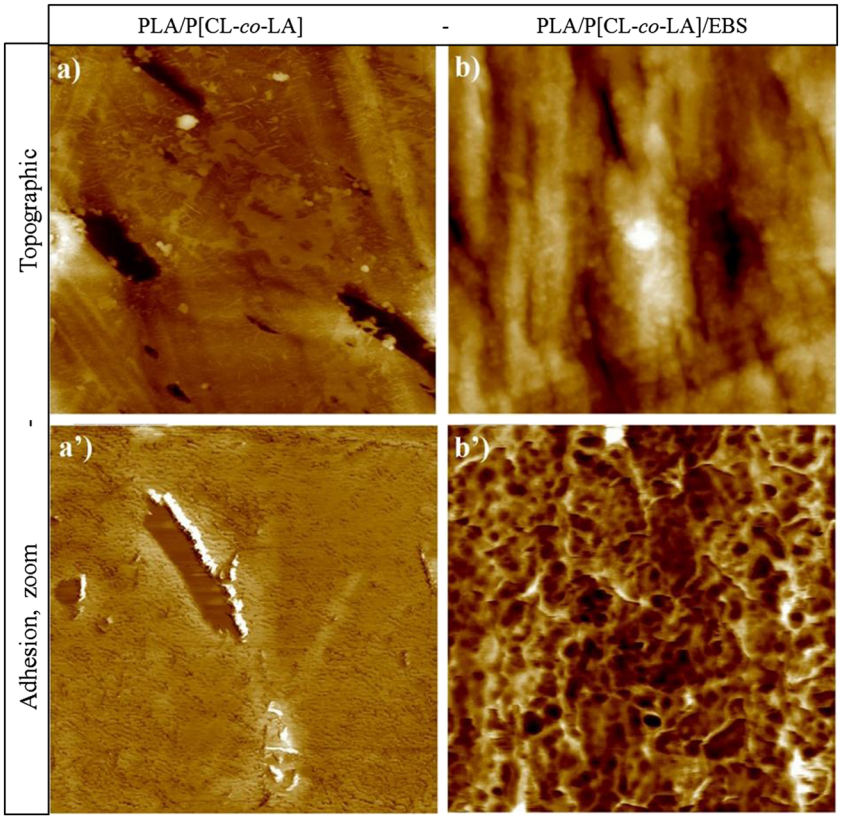

Figure 5. Peak-force tapping atomic force microscopy analysis using topographic (images a and b, 5 μm x 5 μm, Z-ranges of 150 nm) and adhesion (images (a') and (b'), zoom to 2 × 2 μm within the PLA matrix, Z-ranges of 230 nN) imaging of polylactide-based materials containing 10 wt% of P[CL-*co*-LA] (images (a) and (a')) and corresponding blend filled with 3 wt% of EBS (images (b) and (b')). This figure is available in colour online at wileyonlinelibrary.com/journal/pat

Besides the crystallization of the polymer matrix, phase-morphology might also play a decisive role on the final mechanical properties of rubber-toughened PLA. In this respect, a new technique, that is, PFT-AFM was introduced to encompass both morphological and surface features of resulting PLA-based materials (Fig. 5). This technique allows us to locally measure various mechanical properties at nanoscale, such as stiffness, adhesion, deformation, and dissipation, simultaneously to the surface topography with high resolution and minimal damage to the probe or sample.[45] To address this important issue, the effect of EBS has been investigated on the blend morphology of resulting PLA-based materials using PFT-AFM, showing, to some extent, heterogeneous surfaces with non-adhesive and soft-microdomains, which are correlated to the rubbery P[CL-*co*-LA] dispersed phase (Fig. 5). More interestingly, adding the EBS nucleating agent did not promote any alteration of the phase morphology of the rubbery phase within the PLA matrix. However, PFT-AFM measurements clearly evidenced the conversion of amorphous PLA zones into highly crystalline ones in the presence of EBS nucleating agent, that is, the conversion of smooth surfaces into more densely packed and entangled ones (see Fig. 5, adhesion images). Therefore, the earlier results indicates that the addition of EBS into immiscible PLA/P[CL-*co*-LA] blends provides an effective way in extending the PLA crystallization as previously attested by DSC measurements. This so-induced crystallinity extent within the PLA matrix led to the confinement of the P[CL-*co*-LA] dispersed phase among closely packed amorphous regions and improved, to some extent, the compatibility degree between both immiscible polymeric partners (as attested by DMTA, see Figure 2S, *Supporting Information*). From this contribution, the substantial improvement recorded in material performances and toughness upon the EBS concentration can be then strictly attributed to the crystal structure and the enhanced crystallinity extent of resulting PLA-based blends.

From the literature, impact modification of polymers is extensively described based on toughening and fracture mechanisms as called crazing, shear yielding, cavitation, and debonding.[46–50] Typically, PLA deforms through highly localized crazing mechanisms, which is believed to be responsible for its brittle character.[51] In this respect, rubber-modifying PLA[5–8] or extending its crystallization[9–12] are among strategies to undergo one or a combination of greater energy-dissipative toughening mechanisms. For instance, crystal-mediated deformation throughout the matrix is reached upon the extent of PLA crystallinity, involving, to some extent, a significant change in the toughening mechanism from crazing to shear-yielding as crystallization occurs.[22,25] The contribution of the latter is supposed to be the key to achieve desirable toughening performances by dissipating more energy prior to fracture with respect to crazing.[33] In this regard, PLA crystals are believed to provide a path for the propagation of shear-yielding needed for effective energy dissipation through the contribution of spherulitic deformation (inter-spherulitic crack growth and crack growth through spherulites).[13,21] To support this statement, SEM was used and reported on Fig. 6, highlighting high deformations and plasticity within room-temperature fractured surfaces of these PLA-based materials. As previously discussed, the extent of PLA crystallinity represents a promising way to enlarge plastic deformation throughout the matrix, dissipating the fracture energy through shear yielding in the crystalline zones and crazing in the amorphous zones. In this present work, macroscopic localized zones

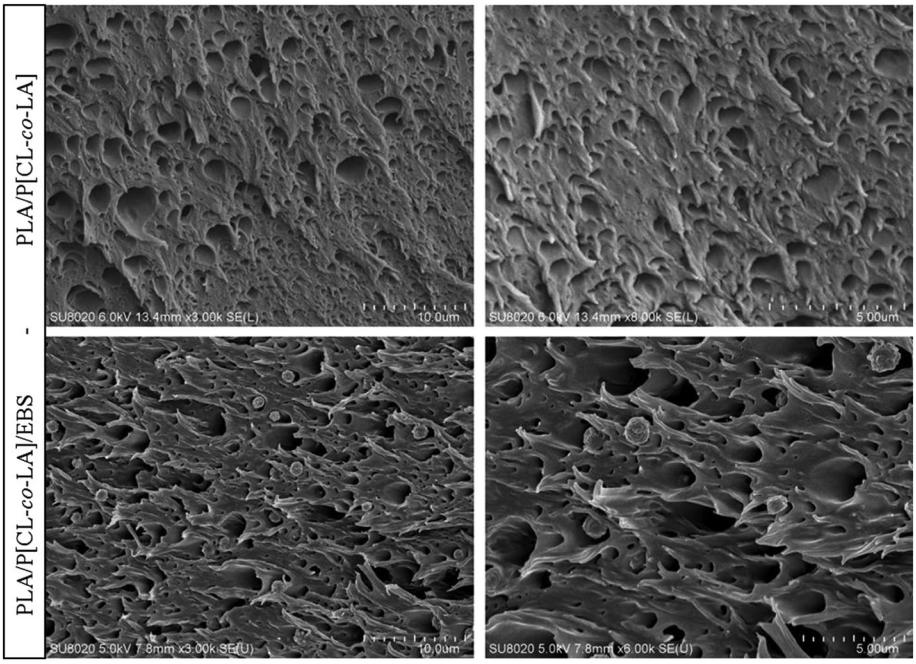

Figure 6. Scanning electron microscopy micrographs (scale of 10 μm on left and zoom to 5 μm on right) of notched surfaces of polylactide-based materials containing 10 wt% of P[CL-*co*-LA] (up) and corresponding blend filled with 3 wt% of EBS (down).

of micro-voids and micro-fibrils which are believed to come from crazing process on deformation are found after the addition of a rubbery P[CL-*co*-LA] impact modifier within the PLA matrix (see Fig. 6, top). However, large-scale plastic deformation and high energy dissipation through a combination of both multiple crazing and shear-yielding within amorphous and crystalline zones, respectively, are expected in the presence of EBS nucleating agent. SEM analysis along the draw axis on deformed samples confirmed the presence of these specific deformations (see Fig. 6, bottom). These features therefore support the statement that loading EBS nucleating agent within PLA-based materials gave rise to largely improved toughness through a change in the deformation mechanism from crazing to shear yielding or a combination of both micromechanisms as crystallization occurs. At this stage, it can be claimed out that the significant crystallization-induced toughness upon the EBS concentration is originated from the crystal structure change of as-converted highly crystalline PLA matrix and the related confinement of the P[CL-*co*-LA] dispersed phase among closely packed amorphous regions, which allowed a combination of multiple crazing and shear-yielding mechanisms. This owes to the fracture energy dissipation throughout the material as follows. (i) When subjected to an external impact force, the closely packed dispersed P[CL-*co*-LA] phase is believed to locally concentrate the stress within the amorphous regions to finally release the hydrostatic strain energy where craze initiation takes place. (ii) This multiple crazing occurs throughout a comparatively large volume of the rubber-modified material, consuming the predominant part of fracture energy. (iii) Besides craze growth, shear band nucleation is affected by the as-released hydrostatic tension in the surrounding rubbery dispersed phase. (iv) This therefore favors shear-yielding through crystal-mediated deformation within highly crystalline regions, leading to a combination of both multiple crazing and shear-yielding within the resulting PLA-based materials. In a toughening perspective, new evidences to account for the as-proposed toughening mechanisms will undoubtedly take part in our next contribution.

Based on this contribution, the significant improved PLA crystallinity extent upon the addition of EBS nucleating agent might help to tailor the phase morphology, even during a high-shearing process such as injection molding. Interestingly enough, our previous contribution highlighted peculiar morphologies (from large droplets to small and long ribbons and the formation of interconnected or even co-continuous networks) as mediated by the addition of silica nanoparticles, following a two-step process and compression molding.[52] However, high shearing undergone through the high-pressure injection of such materials altered the morphology and therefore the resulting toughness. Therefore, in an effort to overcome this limitation, a new investigation regarding the co-addition of silica nanoparticles together with EBS nucleating agent has been attempted in relation with the type of molding techniques, that is, via melt injection or compression molding. Surprisingly, loading 4 wt% of EBS and 5 wt% of nanosilica (CAB-O-SIL M-5) within PLA/P[CL-*co*-LA] (10 wt%) blends (under the same processing conditions as described in the Experimental Section) provided a significant improvement in toughness whichever the shaping procedure, that is, injection or compression molding. No break of the specimen sample could be even recorded under compression molding, while an impact strength as high as 17.8 kJ/m^2 was determined after injection molding. Such a large increase in PLA impact strength is to be related to the combination effect of nanosilica and EBS nucleating agent, that is, compatibilization at the PLA/P[CL-*co*-LA] interface and tuning of PLA crystallinity, respectively.

CONCLUSIONS

Developing novel strategies to simultaneously improve the toughness and the crystallinity extent of PLA-based materials is gaining a significant importance, in order to enlarge the range of applications for this renewable polymer. In this respect, co-adding 10 wt% of rubber-like P[CL-*co*-LA] impact modifier and

different concentrations of EBS nucleating agent within PLA led to crystallization-induced toughness as attested by the 11-fold increase in impact strength with respect to neat PLA (i.e., 30.5 kJ/m^2 vs. 2.7 kJ/m^2). The result showed a clear relationship between the overall toughening performance and the outstanding crystallization properties (i.e., matrix crystallinity, spherulitic growth rate, and crystal structure) of resulting PLA-based materials. For instance, the conversion of amorphous PLA zones into highly crystalline ones (i.e., passing from smooth surfaces into more densely packed and entangled ones) was reported owing to PFT-AFM measurements in the presence of EBS nucleating agent. Another confirmation was obtained from isothermal and non-isothermal DSC measurements, highlighting significant reductions about the crystallization half-time ($t_{1/2}$) and surprising change in the crystallization behavior (e.g., double melting peak is converted into a single one, exothermic crystallization peak on cooling, decrease of the cold crystallization enthalpy, *etc.*) upon the EBS content. Using POM analysis, it was further found that loading EBS nucleating agent within immiscible PLA/P[CL-*co*-LA] blends led to crystal structure changes, while their progressive entanglements and growth thereby took part in the large nuclei density achieved upon the EBS concentration. These results clearly confirm that EBS behaves as a remarkable nucleating agent for PLA-based materials. However, adding EBS nucleating agent did not promote any alteration of phase morphology of the rubbery phase within the PLA matrix. Therefore, the earlier results imparted the substantial difference in the toughness extent upon the EBS content to the PLA matrix crystallization. Crystal-mediated deformation was accordingly reached within such PLA-based materials, promoting high energy dissipation through a combination of multiple crazing and shear-yielding as crystallization occurs. As-induced shear yielding in the crystalline zones thereby triggers effective high-impact energy dissipation and promotes the overall material crystallinity as a promising way to enlarge plastic deformation throughout the matrix. Accordingly, a fine tuning of the crystallization behavior of PLA matrix is required for endowing PLA-based materials with new mechanical performances and significant toughening effect. Surprisingly, the phase morphology as mediated by the selective location of nanosilica at the PLA/P[CL-*co*-LA] interface (ribbons and interconnected or even co-continuous structures) might be tailored whichever the shaping procedure (injection or compression molding) in the presence of EBS nucleating agent. Accordingly, a large increase in PLA impact strength was recorded and related to the synergistic effect of nanosilica and EBS nucleating agent, that is, compatibilization at the PLA/P[CL-*co*-LA] interface and tuning of PLA crystallinity, respectively. In this respect, a joint-research with Pukanszky *et al.* will be proposed to implement new evidences about the co-effect of crystallinity and compatibilization way through different processing techniques.

Acknowledgements

This research has been funded by the European Commission and Région Wallonne FEDER program in the frame of "Pôle d'Excellence Materia Nova" and OPTI^{2}MAT program of excellence, by the Interuniversity Attraction Poles program initiated by the Belgian Federal Science Policy Office (PAI P7/05) and by FNRS-FRFC. J. Odent thanks F.R.I.A. for its financial support thesis grant. J-M. Raquez and Ph. Leclère are research associate and senior research associate from F.R.S.-FNRS (Belgium), respectively. Franck Lauro is "Professeur des Universités" at UVHC.

REFERENCES

[1] K. Madhavan Nampoothiri, N. R. Nair, R. P. John, *Bioresour. Technol.* **2010**; *101*, 8493.
[2] R. Auras, B. Harte, S. Selke, *Macromol. Biosci.* **2004**; *4*, 835.
[3] A. Södergård, M. Stolt, *Prog. Polym. Sci.* **2002**; *27*, 1123.
[4] R. M. Rasal, A. V. Janorkar, D. E. Hirt, *Prog. Polym. Sci.* **2010**; *35*, 338.
[5] K. S. Anderson, K. M. Schreck, M. A. Hillmyer, *Polym. Rev.* **2008**; *48*, 85.
[6] S. Ishida, R. Nagasaki, K. Chino, T. Dong, Y. Inoue, *J. Appl. Polym. Sci.* **2009**; *113*, 558.
[7] L. Mascia, M. Xanthos, *Adv. Polym. Tech.* **1992**; *11*, 237.
[8] H. Liu, J. Zhang, *J. Polym. Sci., Part B: Polym. Phys.* **2011**; *49*, 1051.
[9] G. Perego, G. D. Cella, C. Bastioli, *J. Appl. Polym. Sci.* **1996**; *59*, 37.
[10] L. Yu, H. Liu, F. Xie, L. Chen, X. Li, *Polymer Engineering & Science* **2008**; *48*, 634.
[11] J. Gamez-Perez, J. C. Velazquez-Infante, E. Franco-Urquiza, P. Pages, F. Carrasco, O. O. Santana, M. L. Maspoch. *eXPRESS Polymer Letters*, **2011**, 5–82.
[12] S.-D. Park, M. Todo, K. Arakawa, *J. Mater. Sci.* **2004**; *39*, 1113.
[13] S. D. Park, M. Todo, K. Arakawa, M. Koganemaru, *Polymer* **2006**; *47*, 1357.
[14] L. Nascimento, J. Gamez-Perez, O. O. Santana, J. I. Velasco, M. L. Maspoch, E. Franco-Urquiza, *Journal of Polymers and the Environment* **2010**; *18*, 654.
[15] H. T. Oyama, *Polymer* **2009**; *50*, 747.
[16] J. Gamez-Perez, *eXPRESS Polymer Letters* **2010**; *5*, 82.
[17] Z. Tang, C. Zhang, X. Liu, J. Zhu, *J. Appl. Polym. Sci.* **2012**; *125*, 1108.
[18] F. Yu, T. Liu, X. Zhao, X. Yu, A. Lu, J. Wang, *J. Appl. Polym. Sci.* **2012**; *125*, E99.
[19] Z. Gui, C. Lu, S. Cheng, *Polymer Testing* **2013**; *32*, 15.
[20] A. Shakoor, N. L. Thomas, *Polymer Engineering & Science* **2014**; *54*, 64.
[21] J. L. Way, J. R. Atkinson, J. Nutting, *J. Mater. Sci.* **1974**; *9*, 293.
[22] A. C. Renouf-Glauser, J. Rose, D. F. Farrar, R. E. Cameron, *Biomaterials* **2005**; *26*, 5771.
[23] N. Kawamoto, A. Sakai, T. Horikoshi, T. Urushihara, E. Tobita, *J. Appl. Polym. Sci.* **2007**; *103*, 244.
[24] A. M. Harris, E. C. Lee, *J. Appl. Polym. Sci.* **2008**; *107*, 2246.
[25] H. Bai, H. Xiu, J. Gao, H. Deng, Q. Zhang, M. Yang, Q. Fu, *ACS Appl. Mater. Interfaces* **2012**; *4*, 897.
[26] H. Bai, C. Huang, H. Xiu, Y. Gao, Q. Zhang, Q. Fu, *Polymer* **2013**; *54*, 5257.
[27] T. Baouz, F. Rezgui, U. Yilmazer, *J. Appl. Polym. Sci.* **2013**; *128*, 3193.
[28] H. Li, M. A. Huneault, *Polymer* **2007**; *48*, 6855.
[29] S. Jain, M. M. Reddy, A. K. Mohanty, M. Misra, A. K. Ghosh, *Macromol. Mater. Eng.* **2010**; *295*, 750.
[30] K. Hashima, S. Nishitsuji, T. Inoue, *Polymer* **2010**; *51*, 3934.
[31] C. B. Bucknall, *J. Polym. Sci., Part B: Polym. Phys.* **2007**; *45*, 1399.
[32] J. Z. Liang, R. K. Y. Li, *J. Appl. Polym. Sci.* **2000**; *77*, 409.
[33] R. A. C. Deblieck, D. J. M. van Beek, K. Remerie, I. M. Ward, *Polymer* **2011**; *52*, 2979.
[34] J. Odent, P. Leclère, J.-M. Raquez, P. Dubois, *Eur. Polym. J.* **2013**; *49*, 914.
[35] M. Murariu, A.-L. Dechief, R. Ramy-Ratiarison, Y. Paint, J.-M. Raquez, P. Dubois, *Nanocomposites* **2014**; *1*, 1. http://dx.doi.org/10.1179/2055033214Y.0000000008
[36] "PeakForce QNM: Quantitative Nanomechanical Property Mapping", Bruker Applications Note **2011**; http://www.bruker.com/fileadmin/user_upload/8-PDF-Docs/SurfaceAnalysis/AFM/Brochures/PeakForce_Quantitative_Nanomechanical_Property_Mapping_b.pdf (02/02/2015)
[37] H. Fang, Y. Zhang, J. Bai, Z. Wang, *Macromolecules* **2013**; *46*, 6555.
[38] F. Sakai, K. Nishikawa, Y. Inoue, K. Yazawa, *Macromolecules* **2009**; *42*, 8335.
[39] Z. Su, Q. Li, Y. Liu, G.-H. Hu, C. Wu, *J. Polym. Sci., Part B: Polym. Phys.* **2009**; *47*, 1971.
[40] J. Zhang, K. Tashiro, H. Tsuji, A. J. Domb, *Macromolecules* **2008**; *41*, 1352.
[41] M. Yasuniwa, K. Sakamo, Y. Ono, W. Kawahara, *Polymer* **2008**; *49*, 1943.
[42] M. L. Di Lorenzo, M. Cocca, M. Malinconico, *Thermochimica Acta* **2011**; *522*, 110.
[43] S. Saeidlou, M. A. Huneault, H. Li, C. B. Park, *Prog. Polym. Sci.* **2012**; *37*, 1657.
[44] C. Grein, C. J. G. Plummer, H. H. Kausch, Y. Germain, P. Béguelin, *Polymer* **2002**; *43*, 3279.

[45] M. Tielemans, P. Roose, C. Ngo, R. Lazzaroni, P. Leclère, *Prog. Org. Coat.* **2012**; *75*, 560.
[46] W. G. Perkins, *Polymer Engineering & Science* **1999**; *39*, 2445.
[47] R. M. Ikeda, *J. Appl. Polym. Sci.* **1993**; *47*, 619.
[48] P. A. O'Connell, G. B. McKenna, Yield and crazing in polymers, In: *Encyclopedia of Polymer Science and Technology*, John Wiley & Sons, Inc., **2002**.
[49] I. Narisawa, A. Yee, Crazing and fracture of polymers., In: *Materials Science and Technology*, Wiley-VCH Verlag GmbH & Co, KGaA, **2006**.
[50] D. K. Mahajan, A. Hartmaier, *Physical Review E* **2012**; *86*, 021802.
[51] G. Stoclet, J. M. Lefebvre, R. Séguéla, C. Vanmansart, *Polymer* **2014**; *55*, 1817.
[52] J. Odent, Y. Habibi, J.-M. Raquez, P. Dubois, *Compos. Sci. Technol.* **2013**; *84*, 86.